ACS SENSORS

pubs.acs.org/acssensors

Article

An Ultrasensitive Nucleic Acid Detection Platform Based on Phosphorothioate-DNA

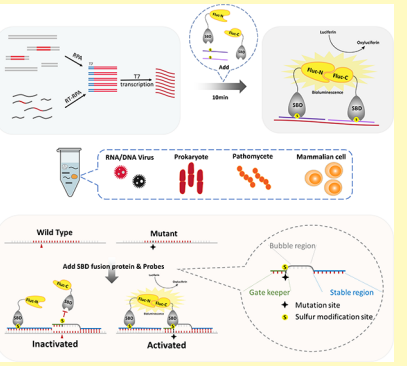
Hang Gao,[†] Yuting Shuai,[†] Yiyi Zheng, Anan Xu, Zhaoxi Han, Dini Ma, Zixin Deng, Xinyi He,* and Guang Liu*

Cite This: https://doi.org/10.1021/acssensors.5c01987

Read Online

ACCESS | Metrics & More | Article Recommendations | Supporting Information

ABSTRACT: Nucleic acid detection plays an essential role in disease diagnosis and epidemic control. Traditional techniques face challenges such as time-consuming procedures and limited accuracy. Despite progress in programmable nuclease systems such as CRISPR and Argonaute, there has been relatively limited exploration of nucleic acid detection methods utilizing DNA modifications. We have previously developed SENSOR (sulfur DNA-mediated nucleic acid sensing platform) for rapid detection of single-stranded DNA (ssDNA) by employing phosphorothioate (PT) modification and sulfur binding domains (SBDs). Here we present SENSOR 2.0, which has been expanded to detect RNA at single-copy level sensitivity. In addition, using a Bubble-Probe design, SENSOR 2.0 is capable of distinguishing single nucleotide variations (SNVs). In 57 clinical *Candida albicans* samples, the azole drug-resistant point mutation in the *ERG11* gene was successfully identified with SENSOR 2.0. These results establish SENSOR 2.0 as an innovative and highly effective technique for nucleic acid detection.



KEYWORDS: *nucleic acid detection, single nucleotide variations, phosphorothioate, sulfur binding domain, Bubble-Probe*

Downloaded via SHENZHEN UNIV on October 30, 2025 at 01:56:40 (UTC).
See https://pubs.acs.org/sharingguidelines for options on how to legitimately share published articles.

Over the past decade, epidemic outbreaks caused by pathogens including bacteria, fungi, and viruses have emphasized the requirement for rapid, convenient, and sensitive nucleic acid detection techniques. The "gold standard" qPCR method for routine clinical diagnosis is complicated, time-consuming and requires expensive equipment.[1] Isothermal amplification methods like loop-mediated isothermal amplification (LAMP)[2] and recombinase polymerase amplification (RPA)[3] are relatively deficient in sensitivity and specificity. Recently, programmable nucleases including clustered regularly interspaced short palindromic repeats (CRISPR) and Argonaute have revolutionized the fields of gene editing and nucleic acid detection, such as DETECTR, SHERLOCK, HOLMES, RADAR and MULAN technologies.[4−13] However, CRISPR-Cas and Argonaute technologies face limitations. For example, CRISPR needs PAM sites and expensive crRNA and RNase inhibitors, while Argonaute generally requires high temperature and costly 5′ phosphorylation on the guide ssDNA. Therefore, there is a requirement for an innovative nucleic acid detection technology that is highly sensitive, rapid, cost-effective, easy to operate, and capable of identifying infectious diseases and single nucleotide variants (SNVs).

DNA phosphorothioate (PT) modification, also referred to as DNA sulfur modification, is a unique modification that occurs in the DNA backbone. In PT-DNA, a nonbridging oxygen atom is replaced with a sulfur atom in the phosphodiester bond.[14] PT modification plays a significant role in a range of biological functions, including restriction-modification systems, bacterial defense mechanisms, antioxidant function, and epigenetic regulation.[15] In our previous study, we discovered the PT-dependent restriction endonucleases, which specifically target PT-DNA with the sulfur binding domain (SBD), and make double-strand breaks at 5−30 bases from the PT site.[16−18] We also elucidated that SBD specifically binds PT-DNA by embedding the sulfur atom into a hydrophobic surface cavity and forming hydrophobic interactions.[19−21] PT-DNA has a much stronger affinity with SBD (K_D = 0.005−0.1 μM) than other modifications with their recognition proteins (e.g., the K_D of 5mC-DNA and SRA is about 0.2 ∼ 10 μM).[21−24] This may be due to the fact that PT modifications on the DNA backbone are more accessible to proteins than nucleotide modifications. In addition, unlike DNA methylation, which is ubiquitous across all kingdoms of life, PT-DNA is found only in certain prokaryotes, making it a promising candidate for novel biotechnological applications avoiding interference from native modifications.[25,26]

Based on the specific binding between SBD and PT-DNA, we have developed SENSOR (sulfur DNA mediated nucleic acid sensing platform).[27] In this system, SBD was coupled with the

Received: June 8, 2025
Revised: September 5, 2025
Accepted: October 21, 2025

© XXXX American Chemical Society

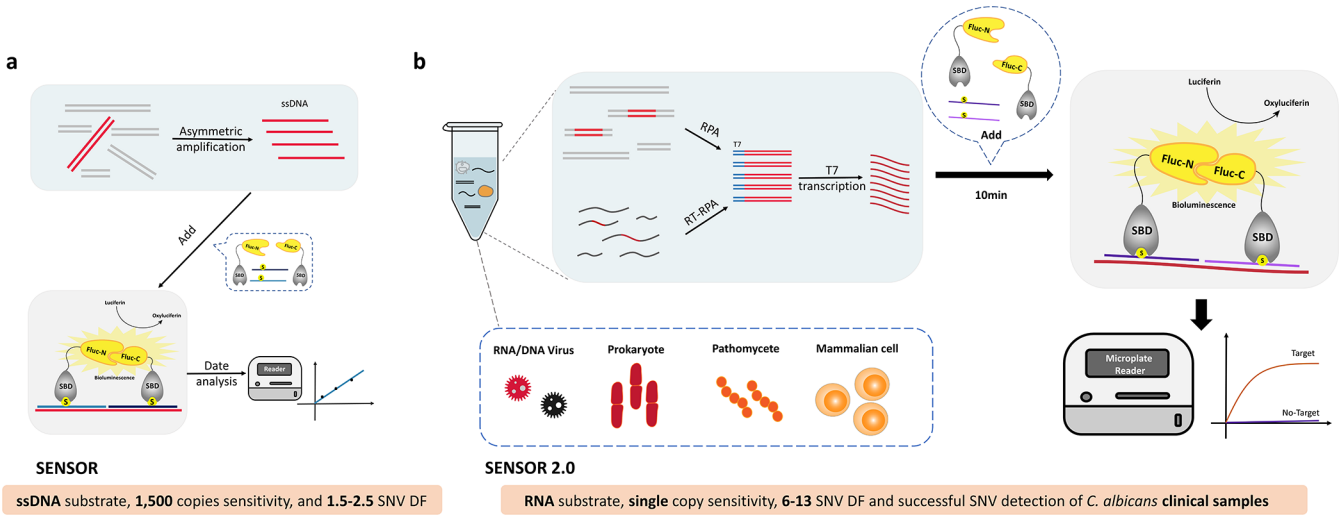


Figure 1. Schematic outline of SENSOR and SENSOR 2.0. SENSOR detects ssDNA samples with a sensitivity of 1500 copies (a), SENSOR 2.0 detects RNA from diverse samples, the detection sensitivity reaches single-copy level, and has a 5-fold increase in SNV discrimination factor (DF) (b).

firefly luciferase split reporter system (Fluc-N and Fluc-C), and two PT-modified probes were used to hybridize with adjacent positions on the target ssDNA. The PT-probes anneal with the target ssDNA and form dsDNA with two PT-sites. Then SBDs bind to the newly formed PT-sites, and a luminescence signal could be generated by the complementation of the split reporter. SENSOR provides insights for research on modification-dependent REases and facilitates biotechnology applications of PT-DNA. However, the current SENSOR system exhibits limitations in analytical sensitivity, substrate scope, and single-nucleotide variant (SNV) discrimination capability, necessitating targeted improvements to broaden its applicability and precision in complex biological matrices.

In this study, we updated SENSOR 2.0, a platform with high sensitivity, the ability to discriminate SNVs and the capability of detecting RNA. Through the screening of various 2′-modified PT-probes, the DNA PT-probe exhibited the highest efficacy in detecting both ssDNA and RNA substrates. By utilizing RPA coupled with *in vitro* transcription (IVT) by T7 RNA polymerase, we have successfully achieved ultrasensitive detection with single-copy sensitivity. With a Bubble-Probe (BP) design, we improved the discrimination factor (DF, which refers to the ability to distinguish wild type and mutant with only a single base difference) of SNVs by 3−6 fold, enabling effective identification of SNVs. In a test involving 57 clinical samples, SNVs within the *ERG11* gene of *Candida albicans* were determined using SENSOR 2.0, resulting in the successful discrimination of wild-type, mutant, and heterozygous genotypes. Our findings present SENSOR 2.0 as a powerful tool for nucleic acid detection in the diagnosis of infectious diseases and SNV identification.

METHODS AND INSTRUMENTS

Reagents and Instruments. Oligonucleotides used in this study were synthesized by Genewiz co. (Suzhou, China) or GenScript (Nanjing, China), with detailed sequences listed in Tables S1 and S2. The plasmids and strains used in this study are listed in Table S3. The Steady-Glo luciferase reporter gene detection system kit was purchased from Promega. The DNA isothermal rapid amplification kit was purchased from Amplification Future (Weifang, China). The HiScribe T7 High Yield RNA Synthesis Kit was purchased from New England Biolabs. The SYBR Gold nucleic acid dye was purchased from Thermo Fisher Scientific Inc. The Taq polymerase was purchased from Takara Bio Inc. The QX200 ddPCR EvaGreen Supermix was purchased from Bio-Rad. The Ni-NTA chromatographic column, PD-10 desalination chromatographic column, and AKTA FPLC system were purchased from Cytiva. All chemicals and reagents used were of analytical grade. The clinical *C. albicans* samples used for SNV detection were provided by the Shanghai Institute of Immunity and Infection. Plasmid construction and protein purification were performed in accordance with previously published methods.[27]

Electrophoretic Mobility Shift Assay (EMSA) of SBD Binding 2′-Modified PT-Probes Annealed with ssDNA or RNA. The 2′-modified PT-probes were annealed with complementary ssDNA or RNA by heating to 95 °C and gradually cooling in 1 × Thermopol Buffer (#B9004S, NEB), yielding 15 bp annealed nucleic acid substrates. The 10 μL reaction mixture of EMSA consisted of 150 pmol SBD_{Mmo}, 7.5 pmol annealed substrate, 160 mM NaCl, 25 mM Tris-HCl (pH 8.0) and 5% glycerol. The mixtures were loaded onto 12% nondenaturing polyacrylamide gels (acrylamide: bis(acrylamide) 79:1, w/w) and subjected to electrophoresis in 0.5 × Tris-borate-EDTA (TBE) buffer at 150 V for 60 min. Subsequently, the gels were stained with SYBR Gold and analyzed using the ChemiDoc XRS Gel Imaging System (Bio-Rad). The binding efficiency was determined by the decrease in substrate band intensity.

Optimization of SENSOR 2.0. In SENSOR 2.0, we reoptimized the detection conditions from SENSOR and investigated several key reaction parameters. Salt concentrations of 40 mM, 80 mM, 160 mM, 240 mM, 320 mM, and 400 mM NaCl were investigated to determine the optimal detection concentration at pH 8.8. The optimal detection pH for RNA was determined by gradient screening of pH 6.5, pH 7.2, pH 8.0, pH 8.8, and pH 9.6 at 160 mM NaCl. Next, we analyzed the influence of recombinant protein ratios on RNA detection, and the molar ratios of SBD_{Mmo}+Fluc-N (M+N) to Fluc-C+SBD_{Mmo} (C+M) were 1:0.2, 1:0.4, 1:0.8, 1:1, 1:2, and 1:4. The optimal detection condition comprised 0.5 pmol of each probe, 0.5 pmol of target ssDNA or RNA, 160 mM NaCl, 25 mM Tris-HCl (pH 8.0), 10 μL of Luciferase Assay Substrate (Promega), and 5 pmol of proteins M+N and C+M each.

Substrate Amplification by RPA Coupled with IVT. The *KatG* gene fragment of *Mycobacterium tuberculosis* and *ORF1ab* gene fragment of SARS-CoV-2 were quantified using digital droplet PCR (ddPCR) following the standard protocol, followed by serial dilution.

The RPA reactions were carried out according to the manufacturer's protocol, with an incubation time of 20 min at 37 °C. Next, 1 μL of the RPA product was transferred to a 9 μL T7 RNA amplification reaction system (4.25 μL of deionized water, 0.75 μL of 10 × reaction buffer, 0.75 μL of each 100 mM NTP, and 1 μL of T7 RNA polymerase mix), and incubated at 37 °C for another 20 min. Finally, 1 μL of T7 transcripts was added to the detection system (0.5 pmol of each probe,

https://doi.org/10.1021/acssensors.5c01987
ACS Sens. XXXX, XXX, XXX−XXX

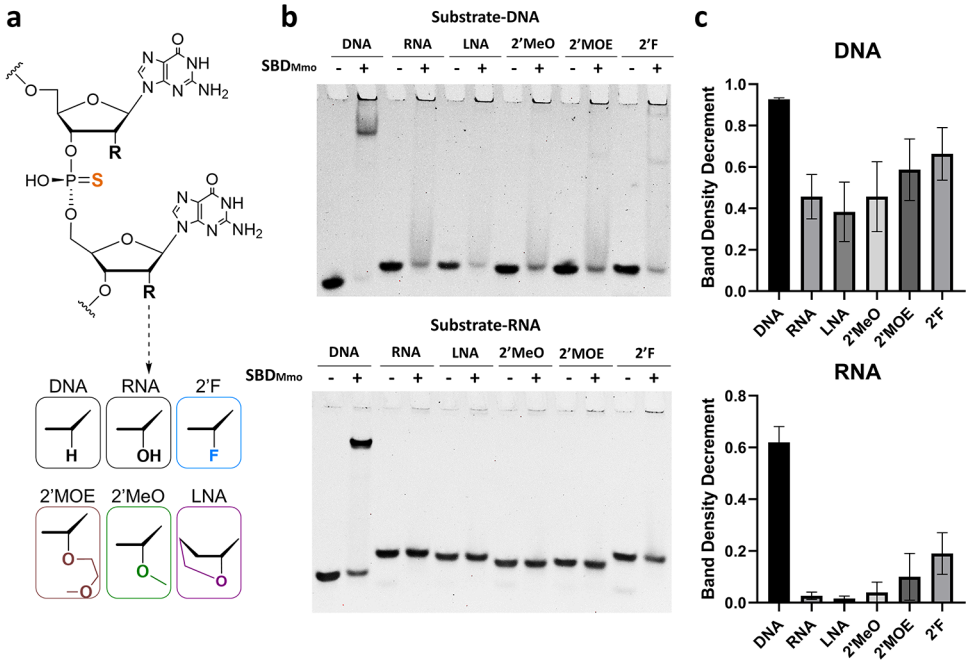


Figure 2. Screening for the optimal PT-probes. (a) The chemical structures of six types of 2′-modified PT-oligonucleotides, which were evaluated as probes for SENSOR 2.0. (b) EMSA analysis of SBD_{Mmo} binding to six 2′-modified PT-probes annealed with ssDNA (upper panel) or RNA (lower panel). (c) Quantitative analysis of the binding efficiency of SBD_{Mmo} on six 2′-modified PT-probes annealed with ssDNA (upper panel) or RNA (lower panel). Error bars represent the standard deviation of three replicates.

160 mM NaCl, 25 mM Tris-HCl pH 8.0, 10 μL Luciferase Assay Substrate (Promega), and 5 pmol of M+N and C+M each). Luminescence was immediately detected at 30 °C for 10 min using a Bio-Tek microplate reader.

SNV Detection. For SNV detection of *C. albicans* (A798C of *ERG11*) and *M. tuberculosis* (G944C of *KatG*), we first used chemically synthesized sequences (Table S2) for BP optimization. Subsequently, a total of 57 clinical samples of *C. albicans* were lysed by Rapid Nucleic Acid Release Reagent (DNA) - Type II (Amp-future, Changzhou, China), and 5 μL of supernatant was used for SNV detection at A798C of *ERG11* using SENSOR 2.0. The results were compared with those obtained via Sanger sequencing.

RESULT AND DISCUSSION

Design of the SENSOR 2.0 System. The SENSOR system has a detection threshold of 1500 copies with asymmetric RPA and 10 copies with asymmetric PCR amplification. In our subsequent investigation, we observed that SBD exhibited a certain degree of binding affinity toward PT-modified RNA.[20] The amplification rate of ssDNA is relatively low, particularly for isothermal amplification. In contrast, RNA substrates can be obtained through the combination of RPA with IVT, leading to a higher amplification rate.[6] In SENSOR 2.0, we screened the optimal modified probes for detection of RNA substrates, instead of ssDNA in SENSOR, to achieve better sensitivity (Figure 1).

The SENSOR system can detect SNVs, but the discrimination factor (DF) is only about 1.5−2.5. Although SBD shows a clear binding preference for dsDNA over ssDNA, it does not display high sensitivity toward DNA mismatches.[27] In SENSOR 2.0, we developed a molecular switch employing Bubble-Probe (BP) that can alternate between ssDNA and dsDNA in response to SNVs. The BP consists of a Bubble region that mismatches with the substrate, a longer Stable region that complements the substrate, and a shorter Gate keeper region containing the SNV site and the PT-modification (refer to Figure 5a). The Stable region binds the substrate specifically and forms a stable double-stranded region. The Gate keeper transitions between single-strand (inactivated) and double-strand (activated) configurations in response to alteration of a single base pair. The Bubble region functions as a barrier, separating the Gate keeper from the Stable region in order to ensure the responsiveness of the Gate keeper (Figure 5b). With the BP design, the Gate keeper forms separated single-stranded DNA and RNA with the wild-type substrate, but double-stranded DNA/RNA duplex with mutant substrate, resulting in discrimination of SNVs.

PT-Probe Screen for RNA Substrate. We first explored the optimal PT-probe for ssDNA and RNA substrates by evaluating six commonly used 2′-modified oligonucleotide types: DNA, RNA, 2′-F, 2′-MOE, 2′-MeO, and LNA (Figure 2a and Table S1). The 2′-modified PT-probes were annealed with ssDNA or RNA substrates and EMSAs were performed to analyze the binding with SBD. As shown in the upper panel of Figure 2b,c, SBD could bind all types of PT-probes hybridized with ssDNA substrate. The DNA PT-probe/ssDNA hybrid exhibited the highest affinity, with over 90% of the control DNA substrate shifted. The annealing products for 2′-F PT-probe and 2′-MeO PT-probe also bound SBD effectively, with 70 and 60% of the substrate shifted compared to the respective control. By contrast, the RNA, LNA, and 2′-MeO PT-probes showed relatively low affinity. With respect to RNA substrates, SBD generally exhibits a lower binding affinity when compared to DNA substrates (Figure 2b,c, lower panel). The DNA PT-probe/RNA hybrid also displays the highest affinity, with over 60% of the control RNA substrate shifted, whereas the other PT-probes showed rather low affinity to SBD. These results indicate that the DNA PT-probe is the most suitable for both ssDNA and RNA substrates.

These results demonstrate that SBD effectively binds PT-dsDNA and PT-DNA/RNA duplex. In contrast, its affinity for other types of double-stranded nucleic acids, such as PT-dsRNA

https://doi.org/10.1021/acssensors.5c01987
ACS Sens. XXXX, XXX, XXX−XXX

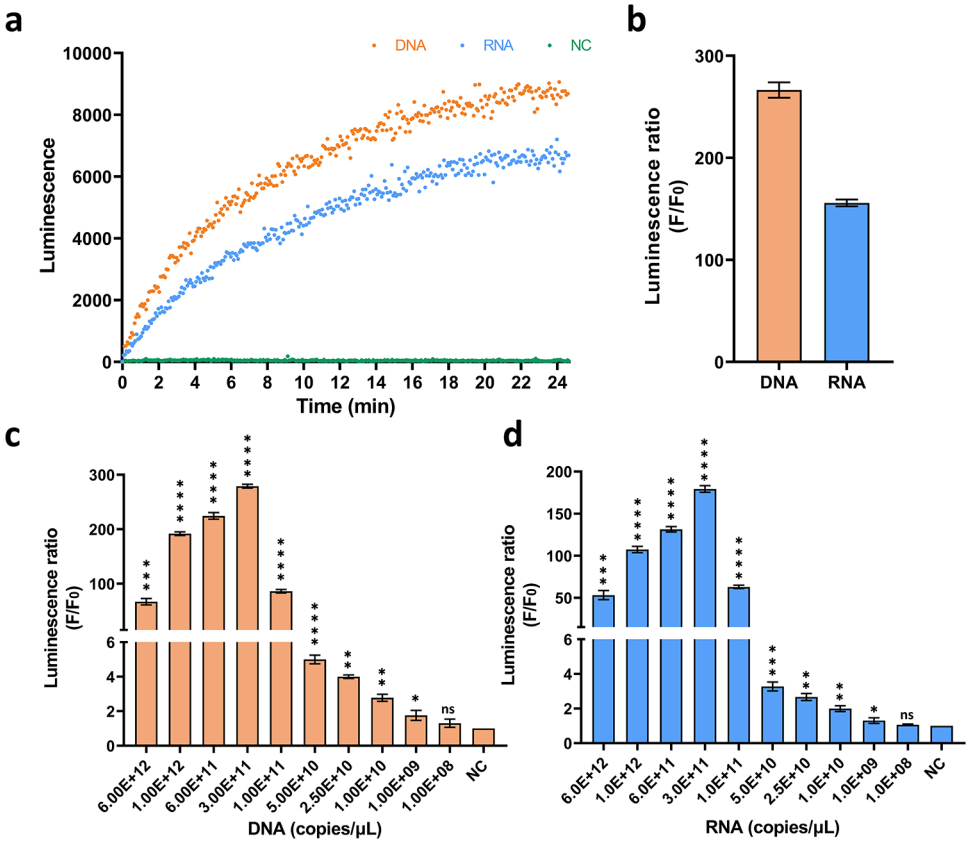


Figure 3. Luminescence intensity curve (a) and Signal-to-Noise Ratio (SNR) (b) for the detection of ssDNA and RNA. F and F_0 denote the luminescence intensity at 10 min in the sample and control groups, respectively. The SNR for detections with serially diluted ssDNA (c) and RNA (d). Statistical significance was determined using a two-tailed Student's *t*-test (*$P < 0.05$, **$P < 0.01$, ***$P < 0.001$, and ****$P < 0.0001$). Error bars indicate the standard deviation of three replicates. All significances were calculated by comparing experimental groups with the negative control group (NC), in which only ddH_2O was added.

or PT-RNA hybrid with DNA (PT-RNA/DNA duplex), is much lower. The structure of SBD binding PT-DNA/RNA duplex was predicted by AlphaFold 3.0 (Figure S1).[28] Since dsDNA typically adopts a B-form structure and dsRNA tends to favor an A-form structure, which is shorter and wider than the canonical B-form,[29] our hypothesis suggests that SBD shows a preference for binding to B-form nucleic acids, particularly for the PT-modified strand.

Optimization of Detection Sensitivity in SENSOR 2.0. Since SBD has an effective binding with PT-DNA/RNA duplex, we decided to employ PT-DNA probes for RNA detection in SENSOR 2.0. We first measured the efficacy of SENSOR on RNA substrates, but the detection yielded a low signal intensity. Therefore, we optimized the pH, salt concentration, and protein ratio in the detection system (Figures S2, S3 and S4). The optimal reaction conditions for SENSOR 2.0 were established at pH 8.0, 160 mM NaCl, and a protein ratio of 1:1 (mol/mol). A typical 20 μL detection system consists of 0.5 pmol of two PT-probes, each containing five PT-modifications, and produces a stable signal within approximately 10 min at room temperature. Compared to the reaction conditions of SENSOR (400 mM NaCl, 25 mM Tris-HCl, pH 8.0), the salt concentration for SENSOR 2.0 decreased to 160 mM NaCl. Since salt ions usually disrupt protein−DNA interactions,[30,31] the affinity of SBD for nucleic acids is increased as the concentration of NaCl decreased from 400 mM (SENSOR) to 160 mM (SENSOR 2.0). EMSA results showed that SBD exhibits lower binding affinity toward PT-DNA/RNA duplex compared to PT-dsDNA. Therefore, a decreased NaCl concentration is recommended to achieve optimal detection of RNA substrate with SENSOR 2.0. Detections of DNA and RNA substrates were carried out under the specified conditions, resulting in a similar detection effect as indicated by the luminescence intensity curves (Figure 3a). SENSOR 2.0 achieved more than a 100-fold signal differentiation between the experimental group (matching sequence) and the control group (deionized water) for both DNA and RNA substrates (Figure 3b). We then prepared a series of ssDNA and RNA sample dilutions to evaluate the sensitivity of SENSOR 2.0 (Figure 3c,d). The detection sensitivity for both ssDNA and RNA substrates was almost the same, at 1×10^9 copies/μL (sample concentration). We observed that the luminescence ratio reached a maximum at a substrate concentration of 3.0×10^{11} copies/μL. Since our approach involves two probes to anneal with the same molecule of substrate, in cases where the substrate concentration exceeds that of the probes, some substrate molecules only anneal with one probe, resulting in a failure to activate the luminescence reporting system and subsequently decreasing the detection signal. In agreement with this, we observed that a higher amount of probes is required for a higher copy number of substrate to achieve the peak signal (Figure S5a,b). However, the background luminescence also rose with increasing probe amounts (Figure S5c), prompting us to opt for 0.5 pmol of probes per reaction for optimal detection sensitivity.

In order to further improve sensitivity, we investigated combining amplification by RPA and IVT in SENSOR 2.0. The

https://doi.org/10.1021/acssensors.5c01987
ACS Sens. XXXX, XXX, XXX−XXX

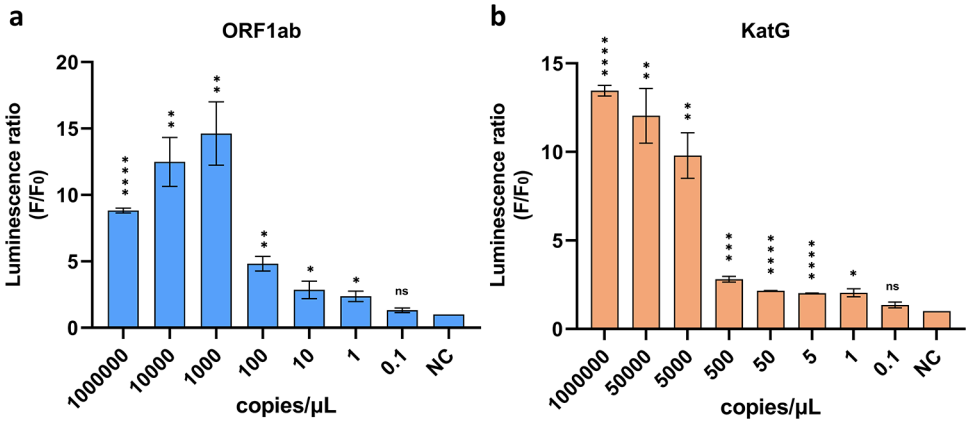


Figure 4. Detection of serial dilutions of the *ORF1ab* gene of SARS-CoV-2 (a) and the *KatG* gene of *M. tuberculosis* (b). F and F_0 represent the luminescence intensity at 10 min in the sample and control groups, respectively. Statistical significance was determined using a two-tailed student's *t*-test (*$P < 0.05$, **$P < 0.01$, ***$P < 0.001$, and ****$P < 0.0001$). Error bars indicate the standard deviation of at least three replicates. All experimental groups were compared with the negative control (NC) group, in which only the amplified product of ddH_2O was added, to determine statistical significance.

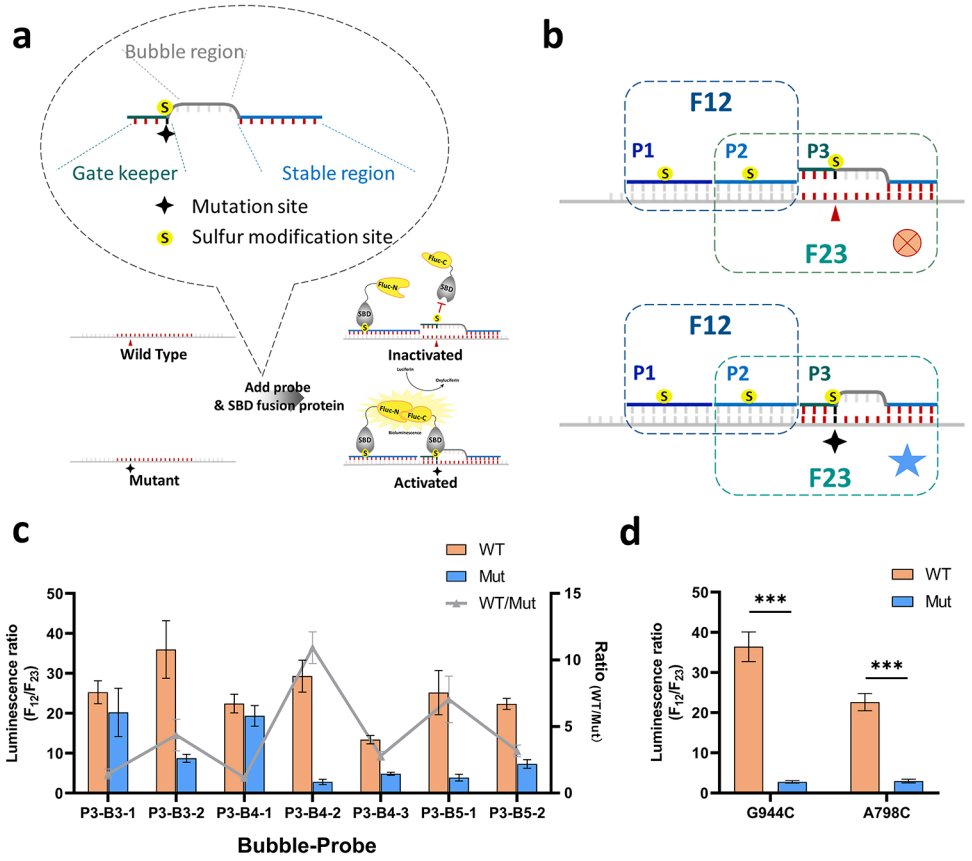


Figure 5. Scheme of SNV detection with SENSOR 2.0. (a) The Bubble-probe P3 was used to construct a molecular switch that shifts from PT-dsDNA to PT-ssDNA upon a single nucleotide alteration. SNV detection was accomplished by discriminating between PT-dsDNA and PT-ssDNA with SBDs. (b) Three adjacent probes, including the Bubble-probe P3, were used for SNV identification, with the luminescence signals of probes P1 and P2 (F_{12}) serving as controls, and the luminescence signals of probes P2 and P3 (F_{23}) used for detection. The wild-type has a high F_{12}/F_{23} ratio, while the mutant has a low F_{12}/F_{23} ratio. (c) Optimization of P3 with varying lengths in the Gate keeper and Bubble regions. (d) SNV detection for *C. albicans* (A798C of *ERG11*) and *M. tuberculosis* (G944C of *KatG*) using SENSOR 2.0. Statistical significance was determined using a two-tailed student's *t*-test (*$P < 0.05$, **$P < 0.01$, ***$P < 0.001$, and ****$P < 0.0001$). Error bars indicate the standard deviation of at least three replicates. The significances were calculated by comparing the SNR of WT and Mut samples.

detection process takes less than 60 min, with 20 min for RPA, 20 min for IVT, and 10 min for probe binding and luminescence generation. We attempted to detect the bacterial and viral pathogens *M. tuberculosis* and SARS-CoV-2 for subsequent investigation. Fragments of the *KatG* gene of *M. tuberculosis* and the *ORF1ab* gene of SARS-CoV-2 were quantified with ddPCR and used as detection targets (Figure S6). Serial dilutions of the detection targets underwent amplification through RPA

https://doi.org/10.1021/acssensors.5c01987
ACS Sens. XXXX, XXX, XXX−XXX

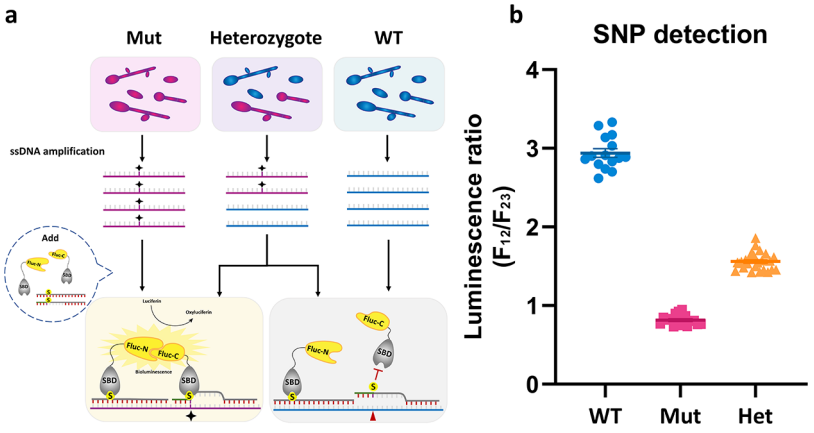


Figure 6. Detection of SNVs in clinical samples of *C. albicans*. (a) The DNA extracted from clinical samples was amplified and then detected using SENSOR 2.0. (b) Detection of SNV (A798C of *ERG11*) in 57 *C. albicans* clinical samples. The 15 samples exhibiting an F_{12}/F_{23} ratio of approximately 3 are categorized as wild-type (WT), the 25 samples showing an F_{12}/F_{23} ratio of around 0.8 are assigned to the mutant (Mut), and the 17 samples with an F_{12}/F_{23} ratio of around 1.8 are considered to be heterozygotes (Het).

combined with IVT. The amplification products were detected by SENSOR 2.0, and the sensitivity reached single-copy level (Figure 4). The results indicate the broad applicability of SENSOR 2.0 in detecting various pathogenic microorganisms with high sensitivity.

SNV Detection by SENSOR 2.0. In order to achieve high DF detection of SNVs, we incorporated a molecular switch into SENSOR 2.0. The molecular switch was formed by a Bubble-Probe (BP) and the RNA(ssDNA) substrate (Figure 5a). For each sample, luminescence was measured with two sets of probes, probes P1−P2, and probes P2−P3. Probes P1 and P2, which are perfectly complementary to the substrate, serve as the control, while the Bubble-probe P3, which is sensitive to SNVs, is employed together with P2 for SNV identification. The Bubble-probe P3 has three bases complementary to the wild-type and four bases complementary to the mutant, resulting in a low luminescence signal (F_{23}) for the wild-type and a high signal for the mutant (Figure 5b). Therefore, the luminescence ratio (F_{12}/F_{23}) is high for the wild-type and low for the mutant.

The G944C mutation in the catalase peroxidase *KatG*, which is the main cause of *M. tuberculosis* resistance to isoniazid, and the A798C mutation in lanosterol 14α-demethylase *ERG11*, which induces azole drug resistance in *C. albicans* were selected as targets for SNV detection. We screened the lengths of the Gate keeper and the Bubble region, finding that the optimal DF is achieved with a Gate keeper of 4 bp and a Bubble region of 4 bp (Figure 5c and Table S2). We then detected the SNV site, revealing a DF of 13 at the G944C site and a DF of 6 at the A798C site between the mutant and wild-type (Figure 5d). Compared to SENSOR, which has a DF of 1.5−2.5 on SNVs (Figure S7), SENSOR 2.0 shows a nearly 5-fold increase in the DF. These assays demonstrate the ability of SENSOR 2.0 to effectively differentiate between various SNVs.

SNV Detection of *Candida albicans* Clinical Samples with SENSOR 2.0. We employed SENSOR 2.0 to detect the A798C mutation in the *ERG11* gene in clinical samples containing the fungal pathogen *C. albicans*. Clinical samples were obtained from 57 patients (Table S4), then subjected to nucleic acid extraction and amplification. The samples were analyzed using SENSOR 2.0 with BP design (Figure 6a).

Among the 57 samples, 15, 25, and 17 exhibited luminescence ratios of approximately 3, 0.8, and 1.8, respectively (Figure 6b), corresponding to the wild-type, the mutant, and the mixture of wild-type and mutant (heterozygotes). The mutations at this site for these samples were verified with Sanger sequencing (Figure S8), yielding results in agreement with those from SENSOR 2.0. These results suggest that SENSOR 2.0 is capable of detecting SNVs in clinical samples.

CONCLUSIONS

In this study, we developed SENSOR 2.0 for the detection of RNA utilizing SBD and PT-DNA probes. We determined that the PT-DNA probe is optimal for the detection of both ssDNA and RNA substrates. SENSOR 2.0 achieved single-copy sensitivity with the amplification procedure combining RPA and IVT. We enhanced SNV discrimination by nearly 5-fold by utilizing the Bubble-probe design, facilitating the detection of SNVs in 57 clinical samples of *C. albicans*.

SENSOR 2.0 is a versatile nucleic acid detection platform with high-sensitivity and high-specificity. It could reach single-copy level sensitivity within a 60 min time frame at room temperature, with high discrimination on SNVs. SENSOR 2.0 does not require specific sequence motifs such as PAM sites of CRISPR-Cas systems, and the PT-probes can be easily designed for any sequence. Although the luciferase reporting system of SENSOR 2.0 is slightly more expensive than the fluorescent reporters in CRISPR, SENSOR 2.0 utilizes only low-cost PT-probes, rather than expensive RNase inhibitors and crRNAs used in CRISPR, thereby providing economic advantages (Table S5). Our experiments with clinical samples validate the reliability and applicability of SENSOR 2.0, demonstrating its potential for use in biomedical research, clinical diagnostics, infectious disease prevention, and other relevant fields. It is worth noting that SENSOR 2.0 has a maximum signal with substrate amount equal to that of the probes, and this phenomenon has little effect on the detection results. It must be acknowledged that SENSOR 2.0 has certain constraints, including a multistep procedure and the requirement for luminescence detection equipment. Our future research involves optimizing reaction conditions for efficient one-pot detection and exploring diverse split reporters, such as split-β-galactosidase and split-β-lactamase,[32] to facilitate visually observable colorimetric detection.

https://doi.org/10.1021/acssensors.5c01987
ACS Sens. XXXX, XXX, XXX−XXX

■ ASSOCIATED CONTENT

Supporting Information

The Supporting Information is available free of charge at https://pubs.acs.org/doi/10.1021/acssensors.5c01987.

Additional data including the predicted structures, optimization of detection conditions, and sequences of nucleic acids used (PDF)

■ AUTHOR INFORMATION

Corresponding Authors

Xinyi He − *State Key Laboratory of Microbial Metabolism, Joint International Research Laboratory of Metabolic & Developmental Sciences, School of Life Sciences & Biotechnology, Shanghai Jiao Tong University, Shanghai 200240, China;* orcid.org/0000-0002-2336-7222; Email: xyhe@sjtu.edu.cn

Guang Liu − *State Key Laboratory of Microbial Metabolism, Joint International Research Laboratory of Metabolic & Developmental Sciences, School of Life Sciences & Biotechnology, Shanghai Jiao Tong University, Shanghai 200240, China;* orcid.org/0000-0003-0468-1061; Email: jyayann@sjtu.edu.cn

Authors

Hang Gao − *State Key Laboratory of Microbial Metabolism, Joint International Research Laboratory of Metabolic & Developmental Sciences, School of Life Sciences & Biotechnology, Shanghai Jiao Tong University, Shanghai 200240, China*

Yuting Shuai − *State Key Laboratory of Microbial Metabolism, Joint International Research Laboratory of Metabolic & Developmental Sciences, School of Life Sciences & Biotechnology, Shanghai Jiao Tong University, Shanghai 200240, China*

Yiyi Zheng − *State Key Laboratory of Microbial Metabolism, Joint International Research Laboratory of Metabolic & Developmental Sciences, School of Life Sciences & Biotechnology, Shanghai Jiao Tong University, Shanghai 200240, China*

Anan Xu − *State Key Laboratory of Microbial Metabolism, Joint International Research Laboratory of Metabolic & Developmental Sciences, School of Life Sciences & Biotechnology, Shanghai Jiao Tong University, Shanghai 200240, China*

Zhaoxi Han − *State Key Laboratory of Microbial Metabolism, Joint International Research Laboratory of Metabolic & Developmental Sciences, School of Life Sciences & Biotechnology, Shanghai Jiao Tong University, Shanghai 200240, China*

Dini Ma − *State Key Laboratory of Microbial Metabolism, Joint International Research Laboratory of Metabolic & Developmental Sciences, School of Life Sciences & Biotechnology, Shanghai Jiao Tong University, Shanghai 200240, China*

Zixin Deng − *State Key Laboratory of Microbial Metabolism, Joint International Research Laboratory of Metabolic & Developmental Sciences, School of Life Sciences & Biotechnology, Shanghai Jiao Tong University, Shanghai 200240, China*

Complete contact information is available at: https://pubs.acs.org/10.1021/acssensors.5c01987

Author Contributions

†H.G. and Y.S. contributed equally to this work. The manuscript was written through contributions of all authors. All authors have given approval to the final version of the manuscript.

Funding

This work was supported by the National Key Research and Development Program of China (2020YFA0907200), National Natural Science Foundation of China (32170047, 32501328); Natural Science Foundation of Shanghai (24ZR1436300), Shanghai Pilot Program for Basic Research - Shanghai Jiao Tong University (21TQ1400204), China Postdoctoral Science Foundation(2024M761952), and Shanghai "Super Postdoctoral" Incentive Program (2023416), Postdoctoral Fellowship Program of CPSF (GZC20231598).

Notes

The authors declare the following competing financial interest(s): One China patent on nucleic acid detection with SENSOR system have been filed.

■ ACKNOWLEDGMENTS

We thank Dr. Qian Liu for her valuable comments on this manuscript. We also thank Dr. Changbin Chen from the Shanghai Institute of Immunity and Infection for providing clinical samples. Additionally, we would like to thank the Core Facilities and Technical Service Center for School of Life Sciences and Biotechnology, Shanghai Jiao Tong University for assistance with ddPCR and we are also grateful to Cui Tai for technical support of analyzing data.

■ REFERENCES

(1) Yuen, K. C. J.; Blevins, L. S., Jr.; Findling, J. W. Important Management Considerations in Patients with Pituitary Disorders During the Time of the Covid-19 Pandemic. *Endocr. Pract.* **2020**, *26* (8), 915−922.

(2) Chaouch, M. Loop-mediated isothermal amplification (LAMP): An effective molecular point-of-care technique for the rapid diagnosis of coronavirus SARS-CoV-2. *Rev. Med. Virol.* **2021**, *31* (6), No. e2215.

(3) Zhao, Y.; Chen, F.; Li, Q.; Wang, L.; Fan, C. Isothermal Amplification of Nucleic Acids. *Chem. Rev.* **2015**, *115* (22), 12491−12545.

(4) Chertow, D. S. Next-generation diagnostics with CRISPR. *Science* **2018**, *360* (6387), 381−382.

(5) Knott, G. J.; Doudna, J. A. CRISPR-Cas guides the future of genetic engineering. *Science* **2018**, *361* (6405), 866−869.

(6) Gootenberg, J. S.; Abudayyeh, O. O.; Lee, J. W.; Essletzbichler, P.; Dy, A. J.; Joung, J.; Verdine, V.; Donghia, N.; Daringer, N. M.; Freije, C. A.; Myhrvold, C.; Bhattacharyya, R. P.; Livny, J.; Regev, A.; Koonin, E. V.; Hung, D. T.; Sabeti, P. C.; Collins, J. J.; Zhang, F. Nucleic acid detection with CRISPR-Cas13a/C2c2. *Science* **2017**, *356* (6336), 438−442.

(7) Chen, J. S.; Ma, E.; Harrington, L. B.; Da Costa, M.; Tian, X.; Palefsky, J. M.; Doudna, J. A. CRISPR-Cas12a target binding unleashes indiscriminate single-stranded DNase activity. *Science* **2018**, *360* (6387), 436−439.

(8) Li, S. Y.; Cheng, Q. X.; Wang, J. M.; Li, X. Y.; Zhang, Z. L.; Gao, S.; Cao, R. B.; Zhao, G. P.; Wang, J. CRISPR-Cas12a-assisted nucleic acid detection. *Cell Discovery* **2018**, *4*, No. 20.

(9) Lu, S.; Tong, X.; Han, Y.; Zhang, K.; Zhang, Y.; Chen, Q.; Duan, J.; Lei, X.; Huang, M.; Qiu, Y.; Zhang, D. Y.; Zhou, X.; Zhang, Y.; Yin, H. Fast and sensitive detection of SARS-CoV-2 RNA using suboptimal protospacer adjacent motifs for Cas12a. *Nat. Biomed. Eng.* **2022**, *6* (3), 286−297.

(10) Wang, F.; Yang, J.; He, R.; Yu, X.; Chen, S.; Liu, Y.; Wang, L.; Li, A.; Liu, L.; Zhai, C.; Ma, L. PfAgo-based detection of SARS-CoV-2. *Biosens. Bioelectron.* **2021**, *177*, No. 112932.

(11) Xun, G.; Liu, Q.; Chong, Y.; Guo, X.; Li, Z.; Li, Y.; Fei, H.; Li, K.; Feng, Y. Argonaute with stepwise endonuclease activity promotes specific and multiplex nucleic acid detection. *Bioresour. Bioprocess.* **2021**, *8* (1), No. 46.
(12) Ye, X.; Zhou, H.; Guo, X.; Liu, D.; Li, Z.; Sun, J.; Huang, J.; Liu, T.; Zhao, P.; Xu, H.; Li, K.; Wang, H.; Wang, J.; Wang, L.; Zhao, W.; Liu, Q.; Xu, S.; Feng, Y. Argonaute-integrated isothermal amplification for rapid, portable, multiplex detection of SARS-CoV-2 and influenza viruses. *Biosens. Bioelectron.* **2022**, *207*, No. 114169.
(13) He, Y.; Shao, S.; Chen, J. High-Fidelity Identification of Single Nucleotide Polymorphism by Type V CRISPR Systems. *ACS Sens.* **2023**, *8* (12), 4478−4483.
(14) Wang, L.; Chen, S.; Xu, T.; Taghizadeh, K.; Wishnok, J. S.; Zhou, X.; You, D.; Deng, Z.; Dedon, P. C. Phosphorothioation of DNA in bacteria by dnd genes. *Nat. Chem. Biol.* **2007**, *3* (11), 709−710.
(15) Wang, L.; Jiang, S.; Deng, Z.; Dedon, P. C.; Chen, S. DNA phosphorothioate modification-a new multi-functional epigenetic system in bacteria. *FEMS Microbiol Rev.* **2019**, *43* (2), 109−122.
(16) Liu, G.; Ou, H. Y.; Wang, T.; Li, L.; Tan, H.; Zhou, X.; Rajakumar, K.; Deng, Z.; He, X. Cleavage of phosphorothioated DNA and methylated DNA by the type IV restriction endonuclease ScoMcrA. *PLoS Genet.* **2010**, *6* (12), No. e1001253.
(17) Yu, H.; Liu, G.; Zhao, G.; Hu, W.; Wu, G.; Deng, Z.; He, X. Identification of a conserved DNA sulfur recognition domain by characterizing the phosphorothioate-specific endonuclease SprMcrA from Streptomyces pristinaespiralis. *Mol. Microbiol.* **2018**, *110* (3), 484−497.
(18) Lutz, T.; Czapinska, H.; Fomenkov, A.; Potapov, V.; Heiter, D. F.; Cao, B.; Dedon, P.; Bochtler, M.; Xu, S. Y. Protein Domain Guided Screen for Sequence Specific and Phosphorothioate-Dependent Restriction Endonucleases. *Front. Microbiol.* **2020**, *11*, No. 1960.
(19) Liu, G.; Fu, W.; Zhang, Z.; He, Y.; Yu, H.; Wang, Y.; Wang, X.; Zhao, Y. L.; Deng, Z.; Wu, G.; He, X. Structural basis for the recognition of sulfur in phosphorothioated DNA. *Nat. Commun.* **2018**, *9* (1), No. 4689.
(20) Hu, W.; Yang, B.; Xiao, Q.; Wang, Y.; Shuai, Y.; Zhao, G.; Zhang, L.; Deng, Z.; He, X.; Liu, G. Characterization of a promiscuous DNA sulfur binding domain and application in site-directed RNA base editing. *Nucleic Acids Res.* **2023**, *51* (19), 10782−10794.
(21) Yu, H.; Li, J.; Liu, G.; Zhao, G.; Wang, Y.; Hu, W.; Deng, Z.; Wu, G.; Gan, J.; Zhao, Y. L.; He, X. DNA backbone interactions impact the sequence specificity of DNA sulfur-binding domains: revelations from structural analyses. *Nucleic Acids Res.* **2020**, *48* (15), 8755−8766.
(22) Shuai, Y.; Xu, A.; Li, J.; Han, Z.; Ma, D.; Duan, H.; Wang, X.; Jiang, L.; Zhang, J.; Tan, G. Y.; Liu, X.; Zhao, Y. L.; Tong, Y.; Wang, S.; He, X.; Deng, Z.; Liu, G.; Zhang, L. Profile and relaxation of sequence-specificity of DNA sulfur binding domains facilitate new nucleic acid detection platform. *Sci. Bull.* **2023**, *68* (16), 1752−1756.
(23) Rajakumara, E.; Law, J. A.; Simanshu, D. K.; Voigt, P.; Johnson, L. M.; Reinberg, D.; Patel, D. J.; Jacobsen, S. E. A dual flip-out mechanism for 5mC recognition by the Arabidopsis SUVH5 SRA domain and its impact on DNA methylation and H3K9 dimethylation in vivo. *Genes Dev.* **2011**, *25* (2), 137−152.
(24) Vaughan, R. M.; Rothbart, S. B.; Dickson, B. M. The finger loop of the SRA domain in the E3 ligase UHRF1 is a regulator of ubiquitin targeting and is required for the maintenance of DNA methylation. *J. Biol. Chem.* **2019**, *294* (43), 15724−15732.
(25) Tong, T.; Chen, S.; Wang, L.; Tang, Y.; Ryu, J. Y.; Jiang, S.; Wu, X.; Chen, C.; Luo, J.; Deng, Z.; Li, Z.; Lee, S. Y.; Chen, S. Occurrence, evolution, and functions of DNA phosphorothioate epigenetics in bacteria. *Proc. Natl. Acad. Sci. U.S.A.* **2018**, *115* (13), E2988−E2996.
(26) Nasrullah; Hussain, A.; Ahmed, S.; Rasool, M.; Shah, A. J. DNA methylation across the tree of life, from micro to macro-organism. *Bioengineered* **2022**, *13* (1), 1666−1685.
(27) Shuai, Y.; Ju, Y.; Li, Y.; Ma, D.; Jiang, L.; Zhang, J.; Tan, G.-Y.; Liu, X.; Wang, S.; Zhang, L.; Liu, G. A rapid nucleic acid detection platform based on phosphorothioate-DNA and sulfur binding domain. *Synth. Syst. Biotechnol.* **2023**, *8* (2), 213−219.
(28) Abramson, J.; Adler, J.; Dunger, J.; Evans, R.; Green, T.; Pritzel, A.; Ronneberger, O.; Willmore, L.; Ballard, A. J.; Bambrick, J.; Bodenstein, S. W.; Evans, D. A.; Hung, C. C.; O'Neill, M.; Reiman, D.; Tunyasuvunakool, K.; Wu, Z.; Zemgulyte, A.; Arvaniti, E.; Beattie, C.; Bertolli, O.; Bridgland, A.; Cherepanov, A.; Congreve, M.; Cowen-Rivers, A. I.; Cowie, A.; Figurnov, M.; Fuchs, F. B.; Gladman, H.; Jain, R.; Khan, Y. A.; Low, C. M. R.; Perlin, K.; Potapenko, A.; Savy, P.; Singh, S.; Stecula, A.; Thillaisundaram, A.; Tong, C.; Yakneen, S.; Zhong, E. D.; Zielinski, M.; Zidek, A.; Bapst, V.; Kohli, P.; Jaderberg, M.; Hassabis, D.; Jumper, J. M. Accurate structure prediction of biomolecular interactions with AlphaFold 3. *Nature* **2024**, *630* (8016), 493−500.
(29) Dock-Bregeon, A. C.; Chevrier, B.; Podjarny, A.; Moras, D.; deBear, J. S.; Gough, G. R.; Gilham, P. T.; Johnson, J. E. High resolution structure of the RNA duplex [U(U-A)6A]2. *Nature* **1988**, *335* (6188), 375−378.
(30) Record, M. T., Jr.; Lohman, M. L.; De Haseth, P. Ion effects on ligand-nucleic acid interactions. *J. Mol. Biol.* **1976**, *107* (2), 145−158.
(31) Misra, V. K.; Hecht, J. L.; Sharp, K. A.; Friedman, R. A.; Honig, B. Salt effects on protein-DNA interactions. The λcI repressor and EcoRI endonuclease. *J. Mol. Biol.* **1994**, *238* (2), 264−280.
(32) Wehr, M. C.; Rossner, M. J. Split protein biosensor assays in molecular pharmacological studies. *Drug Discovery Today* **2016**, *21* (3), 415−429.



https://doi.org/10.1021/acssensors.5c01987
ACS Sens. XXXX, XXX, XXX−XXX